# Whole Genome MBD-seq reveals different CpG methylation patterns in Azacytidine-treated Juvenile Myelomonocytic Leukaemia (JMML) patients

Juvenile myelomonocytic leukaemia (JMML) is a rare and severe form of early childhood leukaemia characterized by clonal proliferation of myelomonocytic cells, progressive anaemia, thrombocytopenia, hepatosplenomegaly and increased fetal haemoglobin (HbF) (Chan *et al*, 2009). The only available curative treatment is allogeneic haematopoietic stem cell transplantation (HSCT), but prognosis remains poor (Niemeyer & Kratz, 2008; Locatelli & Niemeyer, 2015). It has previously been shown that aberrant DNA hypermethylation of distinct target genes defines more aggressive variants of JMML (Flotho *et al*, 2007; Furlan *et al*, 2009; Olk-Batz *et al*, 2011; Poetsch *et al*, 2014). Azacytidine (AZA) is a DNA hypomethylating agent recently employed for JMML treatment (Locatelli & Niemeyer, 2015). To evaluate AZA treatment impact on aberrant methylation in JMML, we screened global DNA methylation in 3 JMML patients before and after AZA treatment. We found global DNA hypermethylation in both pre- and post-AZA treated patient samples compared to healthy controls, and a significant, although patient-specific, AZA-induced hypomethylation effect. Furthermore, we identified several differentially methylated coding and non-coding species of RNA, depicting a complex deregulation at different levels of transcription and translation in JMML.

$CD34^+$ cells were isolated from frozen mononuclear cell suspensions. Three JMML patients at both diagnosis (t0 group) and after the third cycle of AZA (t1 group) (Furlan *et al*, 2009) were studied (Table SI); three additional healthy donor (HD) control samples were also included (HD group). Informed consent was obtained from either parents or legal guardians according to the Declaration of Helsinki. Approval for this study was obtained from the Institutional Review Board of the "Bambino Gesù" Children's Hospital, Rome. JMML patients were treated with AZA as a compassionate use. Methods for $CD34^+$ cells isolation, their percentage assessment and genomic DNA extraction and sequence analysis are detailed in Data S1. The complete DNA-seq datasets are available at the European Bioinformatics Institute European Nucleotide Archive (EBI ENA) database (http://www.ebi.ac.uk/ena; accession number: PRJEB19377). Gene lists and ontologies are available in supplemental files.

After Methyl Binding Domain (MBD) sequencing (EBI ENA database; http://www.ebi.ac.uk/ena) we compared t0 and HD groups (File S1), detecting 987 different transcriptional units corresponding to 714 coding and 273 non-coding sequences, mostly hypermethylated in t0 (Fig 1A Panel i, ii). A functional protein association network (STRING; http://string-db.org/) (Szklarczyk *et al*, 2015) identified 18 different pathways possibly impaired by deregulated DNA-methylation (Figure S1; Table I; false discovery rate [FDR] < 0·05). The same analysis on t1 and HD groups identified 643 unique transcriptional units, with 468 coding and 175 non-coding sequences, indicating a strong tendency towards hypermethylation in JMML samples (File S2; Fig 1A Panel i, ii). Again, the functional protein association network identified 10 putative impaired pathways, similarly to t0 vs. HD analysis (Figure S2; Table I; FDR < 0·05), even if DNA hypermethylation after AZA treatment was reduced.

Involvement of membrane elements, such as adhesion molecules, developmental processes and cell cycle-related genes was recurrent in our analysis, meaning that identifying insights of these pathways could help to further enlighten pathogenic mechanisms and novel targets for therapy in JMML.

Unexpectedly, direct comparative methylation analysis of samples obtained at onset of JMML and after AZA treatment (t0 vs. t1) did not show any significant difference (File S3), suggesting a probable unspecific and unique patient-related pharmacological effect, which was also evident when considering single-case analysis (Figure S3; File S4, S5, S6). Notably, 453 differentially methylated coding regions were shared between newly diagnosed JMML and AZA-treated samples compared to HD (Table SII). Additionally, 261 and 15 coding regions with different methylation status were specific for t0 and t1 respectively (Fig 1B Panel i; Table SII). Among non-coding regions, we also found 165 sequences shared between the two groups (Table SII), while 107 and 10 were unique in the t0 vs. HD and t1 vs. HD, respectively (Fig 1B Panel ii; Table SII). Interestingly, 439 coding and 161 non-coding specific genomic regions preserved their hypermethylated status, describing an apparent resistance to AZA treatment (Fig 1B Panel iii, iv; Table SII). We found different non-coding RNA species, such as microRNAs, splicing RNAs, long noncoding RNAs/antisense transcripts (AS) and other nondescript RNA species (Table SII; Supplemental files), identifying a complex deregulation of pre- and post-transcriptional processes in JMML pathogenesis possibly acting in a cooperative way.

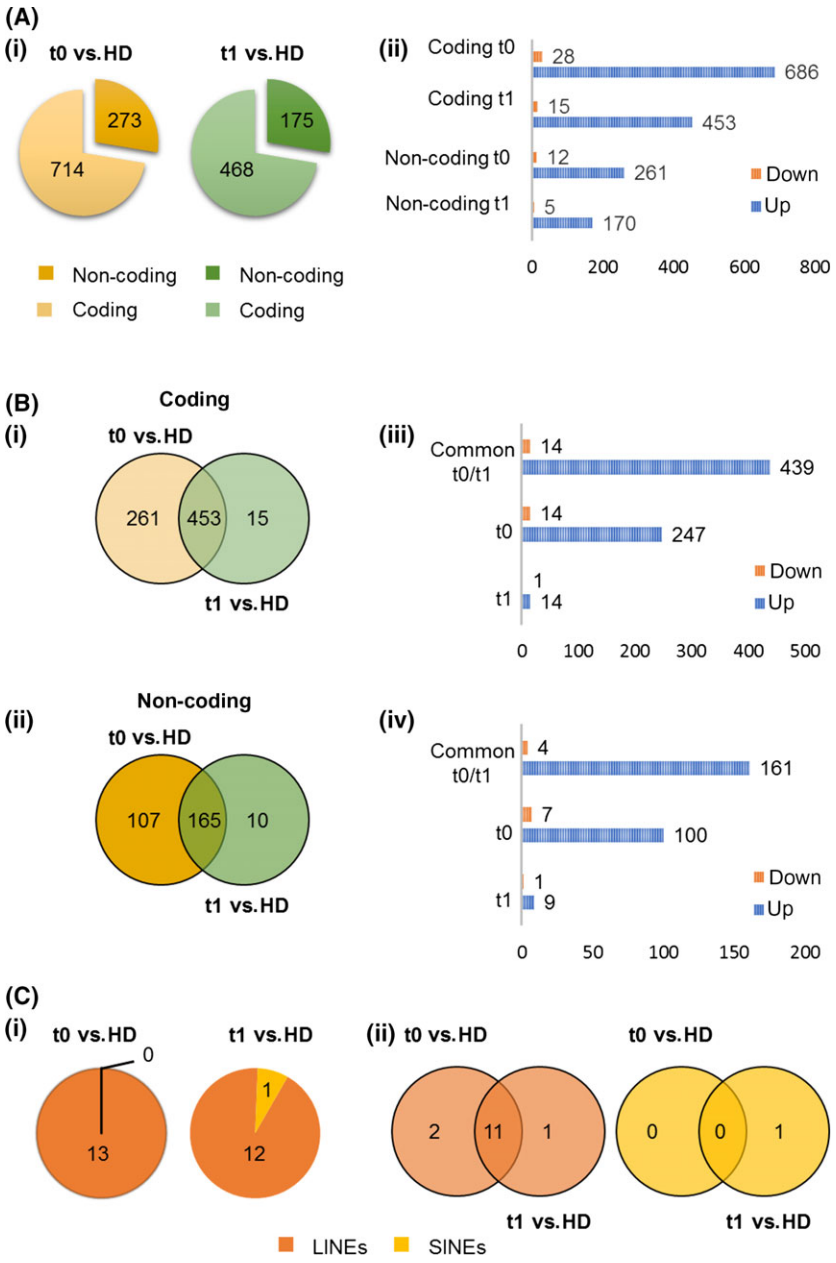


**Fig 1.** Differentially methylated regions in CD34$^+$ cells. (A) Differential methylation sequences abundance is reported for t0 vs. HD analysis on the left and t1 vs. HD analysis on the right panel ($P$ value < 0·05) (i). Bright and dark yellow represent coding and non-coding elements in t0 vs. HD while bright and dark green represent coding and non-coding elements in t1 vs. HD, respectively. Histograms reporting up (blue) and down (orange) methylation trends are showed for both coding and non-coding sequences (ii). (B) Eulero-Venn diagrams represent shared and unique elements in coding and non-coding t0 vs. HD ∩ t1 vs. HD analysis (i and ii). Histograms representing up (blue) and down (orange) methylation trends are showed for both coding (iii) and non-coding sequences (iv) intersection analysis. (C) Abundance of differentially methylated retrotransposons, belonging to LINEs (orange) and SINEs (yellow) families, is reported ($P$ value < 0·05; FDR < 0.05) (i). Eulero-Venn diagrams represent shared and unique retrotransposons in t0 vs. HD ∩ t1 vs. HD analysis for both LINEs and SINEs elements (ii). FDR, false discovery rate; HD, healthy donors; LINEs, long interspersed nuclear elements; SINEs, short interspersed nuclear elements; t0, sample taken at time of diagnosis; t1, sample taken after 3 cycles of azacytidine.

We also screened Long Interspersed Nuclear Elements (LINEs) and Short Interspersed Nuclear Elements (SINEs), due to their correlation with genomic instability, cancer onset and progression (Burns & Boeke, 2012; Hancks & Kazazian, 2016).

We identified 13 LINEs that showed a significant differential methylation profile in t0 with respect to HD (Fig 1C Panel i; File S7). Comparison between t1 and HD revealed the same abundance ($n$ = 13) of differentially methylated retroelements, but they belonged to both LINE and SINE families (Fig 1C Panel i; File S8). Again, a comparison between t0 and t1 groups did not show any significant differentially methylated retrotransposons (File S9). Intersection between the 2 datasets revealed 11 hypermethylated common LINEs (Fig 1C Panel ii). Moreover, all of these 11 LINEs belong to the LINE-1 family and preserve the hypermethylated status compared with HD samples (Table SII; Files S7, S8). Given that LINE-1 elements contain two different promoters with opposite direction, they could drive the transcription of adjacent genes (Hancks & Kazazian, 2016) and their methylation could possibly lead to the inactivation of surrounding genes, suggesting a new potential epigenetic role for retrotransposons in JMML. We also found 2 unique hypomethylated retrotransposons in newly diagnosed JMML and in post-AZA JMML samples in comparison with HD, belonging to the

**Table I.** Pathway networking in t0 vs. HD and t1 vs. HD analysis.

| Pathway category | Pathway ID | Pathway description | Observed gene count | FDR |
|---|---|---|---|---|
| t0 vs. HD | | | | |
| Cellular components | GO.0005887 | Integral component of plasma membrane | 69 | 0·00698 |
| | GO.0008076 | Voltage-gated potassium channel complex | 10 | 0·0219 |
| | GO.0044459 | Plasma membrane part | 88 | 0·0374 |
| Biological processes | GO.0007156 | Homophilic cell adhesion via plasma membrane adhesion molecules | 26 | 1·98e-10 |
| | GO.0098742 | Cell-cell adhesion via plasma-membrane adhesion molecules | 21 | 0·000114 |
| | GO.0048731 | System development | 131 | 0·01 |
| | GO.0016339 | Calcium-dependent cell-cell adhesion via plasma membrane cell adhesion molecules | 7 | 0·0144 |
| | GO.0051094 | Positive regulation of developmental process | 54 | 0·0144 |
| | GO.0007275 | Multicellular organismal development | 143 | 0·0233 |
| | GO.0007399 | Nervous system development | 81 | 0.0243 |
| | GO.0000122 | Negative regulation of transcription from RNA polymerase II promoter | 40 | 0·027 |
| | GO.0007389 | Pattern specification process | 27 | 0·027 |
| | GO.0048568 | Embryonic organ development | 28 | 0·027 |
| | GO.0071883 | Activation of MAPK activity by adrenergic receptor signaling pathway | 3 | 0·027 |
| Molecular function | GO.0005509 | Calcium ion binding | 50 | 7·76e-07 |
| | GO.0000981 | RNA polymerase II transcription factor activity, sequence-specific DNA binding | 33 | 0·0221 |
| | GO.0004938 | alpha2-adrenergic receptor activity | 3 | 0·0221 |
| | GO.1901338 | Catecholamine binding | 5 | 0·0221 |
| t1 vs. HD | | | | |
| Cellular components | GO.0005887 | Integral component of plasma membrane | 48 | 0·0449 |
| Biological processes | GO.0007156 | Homophilic cell adhesion via plasma membrane adhesion molecules | 19 | 1·52e-07 |
| | GO.0098742 | Cell-cell adhesion via plasma-membrane adhesion molecules | 16 | 0·000867 |
| | GO.0051094 | Positive regulation of developmental process | 42 | 0·00349 |
| | GO.0045597 | Positive regulation of cell differentiation | 32 | 0·0214 |
| | GO.0051260 | Protein homooligomerization | 16 | 0·0214 |
| | GO.0007389 | Pattern specification process | 21 | 0·0356 |
| | GO.0000122 | Negative regulation of transcription from RNA polymerase II promoter | 30 | 0·0365 |
| Molecular function | GO.0005509 | Calcium ion binding | 37 | 7·67e-06 |
| | GO.0000981 | RNA polymerase II transcription factor activity, sequence-specific DNA binding | 27 | 0·00484 |

FDR, false discovery rate; HD, healthy donors; t0, sample taken at time of diagnosis; t1, sample taken after 3 cycles of azacytidine.

LINE and SINE family, respectively. (Fig 1C Panel ii; Table SII; File S7, S8, S9).

In conclusion, the whole genome MBD-seq performed on JMML BM-derived $CD34^+$ cells showed a broad genomic hypermethylation in both pre- and post-AZA samples compared to healthy individuals, depicting a novel scenario of pathogenetic epigenetic regulation that is currently poorly understood in JMML. Moreover, a significant patient-specific demethylation AZA impact was detected. The reason for this patient-related response to AZA treatment is still unclear, but we cannot exclude that only those patients exceeding specific levels of hypermethylation may benefit from AZA treatment. Lastly, an intriguing potential role of retrotransposons in JMML should be considered.

## Competing interests

The authors declare no conflict of interests.

## Funding

This work was supported by grants from: AIRC ("My first AIRC" grant 15925 to A.B.; Special Grant "5x1000"-9962 to F.L.) and Ministero della Salute (RF-2011-02350175 to A.B.). P.P.L. is supported by FUV 1693 (Fondazione Umberto Veronesi).

## Acknowledgements

Genomnia s.r.l. for MBD-seq analysis, methods and technical support.

## Authors' contributions

P.P.L., P.V. and A.B. designed the study, wrote the paper, analysed and interpreted data. P.P.L., P.V. and V.T. performed experiments. A.B., M.P.C., A.P., F.D.F. and K.G.

collected samples. F.D.F. collected the data. C.N. and F.L. interpreted data and edited the manuscript.

**Pier Paolo Leoncini**[1]*
**Patrizia Vitullo**[1]*
**Francesca Di Florio**[1]
**Valeria Tocco**[1]
**Maria Giuseppina Cefalo**[1]
**Angela Pitisci**[1]
**Katia Girardi**[1]
**Charlotte Niemeyer**[2]
**Franco Locatelli**[1,3]
**Alice Bertaina**[1]

[1]*Department of Paediatric Haematology and Oncology, Istituto di Ricovero e Cura a Carattere Scientifico (IRCCS) "Bambino Gesù" Children's Hospital, Rome, Italy,* [2]*Department of Paediatrics and Adolescent Medicine, Division of Paediatric Haematology and Oncology Medical Centre, Faculty of Medicine, University of Freiburg, Freiburg, Germany and* [3]*Department of Paediatrics, University of Pavia, Pavia, Italy.*
*E-mail: alice.bertaina@opbg.net*

**These two authors equally contributed as first author.*

**Keywords:** JMML, azacytidine, CpG islands, DNA-methylation, MBD-seq

First published online 2 August 2017
doi: 10.1111/bjh.14876

## Supporting Information

Additional Supporting Information may be found in the online version of this article:

**Fig S1.** Functional protein association network in t0 vs. HD. STRING networks describing the interactions of proteins corresponding to the differentially methylated genes in t0 vs. HD. The color and shape of the arrows show the type of interactions predicted at highest confidence (score $\geq 0.900$). All the gene names and ontologies are reported in supplementary files.

**Fig S2.** Functional protein association network in t1 vs. HD. STRING networks describing the interactions of proteins corresponding to the differentially methylated genes in t1 vs. HD. The color and shape of the arrows show the type of interactions predicted at highest confidence (score $\geq 0.900$). All the gene names and ontologies are reported in supplementary files.

**Fig S3.** Single case differential methylation analysis between pre and post-AZA treatment (t0 vs. t1) in $CD34^+$ cells. (A) Patient 1 differentially methylated sequences abundances including coding (dark grey) and non-coding (light grey) are reported on the left ($P$ Value $< 0.05$). Histogram showing Up (light orange) and Down (dark orange) methylated sequences is also reported on the right. (B) and (C) describes Patient 2 and Patient 3 analysis respectively ($P$ Value $< 0.05$).

**Table SI.** Patients clinical features.

**Table SII.** Common and unique differentially methylated elements in t0 vs. HD and t1 vs. HD analysis.

**Data S1.** Supplementary Methods.

**File S1.** t0 vs. HD genome wide analysis.

**File S2.** t1 vs. HD genome wide analysis.

**File S3.** t0 vs. t1 genome wide analysis.

**File S4.** (Patient 1) t0 vs. (Patient 1) t1 genome wide analysis.

**File S5.** (Patient 2) t0 vs. (Patient 2) t1 genome wide analysis.

**File S6.** (Patient 3) t0 vs. (Patient 3) t1 genome wide analysis.

**File S7.** t0 vs. HD LINE-SINE analysis.

**File S8.** t1 vs. HD LINE-SINE analysis.

**File S9.** t0 vs. t1 LINE-SINE analysis.

## References

Burns, K.H. & Boeke, J.D. (2012) Human transposon tectonics. *Cell*, **11**, 149.

Chan, R.J., Cooper, T., Kratz, C.P., Weiss, B. & Loh, M.L. (2009) Juvenile myelomonocytic leukemia: a report from the 2nd International JMML Symposium. *Leukemia Research*, **33**, 355–362.

Flotho, C., Paulun, A., Batz, C. & Niemeyer, C.M. (2007) AKAP12, a gene with tumour suppressor properties, is a target of promoter DNA methylation in childhood myeloid malignancies. *British Journal of Haematology*, **138**, 644–650.

Furlan, I., Batz, C., Flotho, C., Mohr, B., Lubbert, M., Suttorp, M. & Niemeyer, C.M. (2009) Intriguing response to azacitidine in a patient with juvenile myelomonocytic leukemia and monosomy 7. *Blood*, **113**, 2867–2868.

Hancks, D.C. & Kazazian, H.H. Jr (2016) Roles for retrotransposon insertions in human disease. *Mobile DNA*, **7**, 9.

Locatelli, F. & Niemeyer, C.M. (2015) How I treat juvenile myelomonocytic leukemia. *Blood*, **125**, 1083–1090.

Niemeyer, C.M. & Kratz, C.P. (2008) Paediatric myelodysplastic syndromes and juvenile myelomonocytic leukaemia: molecular classification and treatment options. *British Journal of Haematology*, **140**, 610–624.

Olk-Batz, C., Poetsch, A.R., Nollke, P., Claus, R., Zucknick, M., Sandrock, I., Witte, T., Strahm, B., Hasle, H., Zecca, M., Stary, J., Bergstraesser, E., De Moerloose, B., Trebo, M., van den Heuvel-Eibrink, M.M., Wojcik, D., Locatelli, F., Plass, C., Niemeyer, C.M. & Flotho, C.; European Working Group of Myelodysplastic Syndromes in Childhood. (2011) Aberrant DNA methylation characterizes juvenile myelomonocytic leukemia with poor outcome. *Blood*, **117**, 4871–4880.

Poetsch, A.R., Lipka, D.B., Witte, T., Claus, R., Nollke, P., Zucknick, M., Olk-Batz, C., Fluhr, S., Dworzak, M., De Moerloose, B., Stary, J., Zecca, M., Hasle, H., Schmugge, M., van den Heuvel-Eibrink, M.M., Locatelli, F., Niemeyer, C.M., Flotho, C. & Plass, C. (2014) RASA4 undergoes DNA hypermethylation in resistant juvenile myelomonocytic leukemia. *Epigenetics*, **9**, 1252–1260.

Szklarczyk, D., Franceschini, A., Wyder, S., Forslund, K., Heller, D., Huerta-Cepas, J., Simonovic, M., Roth, A., Santos, A., Tsafou, K.P., Kuhn, M., Bork, P., Jensen, L.J. & von Mering, C. (2015) STRING v10: protein-protein interaction networks, integrated over the tree of life. *Nucleic Acids Research*, **43**, D447–D452.